# Emergence of Spinons in Layered Trimer Iridate math xmlns="http://www.w3.org/1998/Math/MathML" display="inline">mrow>msub>mrow>mi>Ba/mi>/mrow> mrow>mn>4/mn>/mrow>/msub>msub>mrow>mi>Ir/mi> /mrow>mrow>mn>3/mn>/mrow>/msub>msub>mrow>mi mathvariant="normal">O/mi>/mrow>mrow>mn>10/mn>/ mrow>/msub>/mrow>/math>

Y. Shen, J. Sears, G. Fabbris, A. Weichselbaum, W. Yin, H. Zhao, D. G. Mazzone, H. Miao, M. H. Upton, D. Casa, R. Acevedo-Esteves, C. Nelson, A. M. Barbour, C. Mazzoli, G. Cao, and M. P. M. Dean

Phys. Rev. Lett. **129**, 207201 — Published 10 November 2022

DOI: 10.1103/PhysRevLett.129.207201

# Emergence of spinons in layered trimer iridate $Ba_4Ir_3O_{10}$

Y. Shen,[1,*] J. Sears,[1] G. Fabbris,[2] A. Weichselbaum,[1] W. Yin,[1] H. Zhao,[3] D. G. Mazzone,[4] H. Miao,[1,5] M .H. Upton,[2] D. Casa,[2] R. Acevedo-Esteves,[6] C. Nelson,[6] A. M. Barbour,[6] C. Mazzoli,[6] G. Cao,[3] and M. P. M. Dean[1,†]

[1] *Condensed Matter Physics and Materials Science Department, Brookhaven National Laboratory, Upton, New York 11973, USA*
[2] *Advanced Photon Source, Argonne National Laboratory, Argonne, Illinois 60439, USA*
[3] *Department of Physics, University of Colorado Boulder, Boulder, Colorado 80309, USA*
[4] *Laboratory for Neutron Scattering and Imaging, Paul Scherrer Institut, CH-5232 Villigen, Switzerland*
[5] *Material Science and Technology Division, Oak Ridge National Laboratory, Oak Ridge, Tennessee 37830, USA*
[6] *National Synchrotron Light Source II, Brookhaven National Laboratory, Upton, New York 11973, USA*

(Dated: October 18, 2022)

Spinons are well-known as the elementary excitations of one-dimensional antiferromagnetic chains, but means to realize spinons in higher dimensions is the subject of intense research. Here, we use resonant x-ray scattering to study the layered trimer iridate $Ba_4Ir_3O_{10}$, which shows no magnetic order down to 0.2 K. An emergent one-dimensional spinon continuum is observed that can be well-described by XXZ spin-1/2 chains with magnetic exchange of ∼55 meV and a small Ising-like anisotropy. With 2% isovalent Sr doping, magnetic order appears below $T_N$=130 K along with sharper excitations in $(Ba_{1-x}Sr_x)_4Ir_3O_{10}$. Combining our data with exact diagonalization calculations, we find that the frustrated intra-trimer interactions effectively reduce the system into decoupled spin chains, the subtle balance of which can be easily tipped by perturbations such as chemical doping. Our results put $Ba_4Ir_3O_{10}$ between the one-dimensional chain and two-dimensional quantum spin liquid scenarios, illustrating a new way to suppress magnetic order and realize fractional spinons.

Quantum spin liquids (QSLs) are novel states of matter where quantum fluctuations prevent symmetry breaking down to zero temperature [1–6]. A key characteristic of QSLs is that they can host fractional elementary excitations called spinons, carrying spin-1/2, which can serve as a fingerprint for these states. Arguably the best-understood example of this is a one-dimensional (1D) spin-1/2 antiferromagnetic (AFM) chain where the spinons describe the spin domain wall dynamics [7–15]. QSLs in higher dimensions are harder to identify, but hold promise for realizing novel topological order and intrinsic long-range quantum entanglement with potential applications in quantum information [16, 17]. Several studies have provided evidence for spinons in two-dimensional (2D) or three-dimensional (3D) systems such as triangular, Kagome, Kitaev honeycomb, or pyrochlore lattices [18–23], while definitive material-realization remains controversial and is a major target of research. Another possible approach relies on 1D systems as building blocks to realize higher-dimensional QSL states [24], which, however, is less explored.

The insulating magnet $Ba_4Ir_3O_{10}$ is an intriguing candidate for realizing novel mechanisms for the emergence of spinons [25–28]. As shown in Fig. 1(a), it has a quasi-2D structure composed of buckled sheets with a Ir $5d^5$ nominal atomic configuration. Each sheet constitutes corner-connected $Ir_3O_{12}$ trimers containing three distorted face-sharing $IrO_6$ octahedra. The shortest Ir-Ir bond is the one between Ir1 and Ir2 within a trimer, which has a length of ∼2.58 Å [25, 29], shorter than that of elemental iridium (∼2.71 Å [30]). Thus, strong intra-trimer couplings are expected, such as those found in other face-sharing iridates [31–34], and iso-structural $Ba_4Ru_3O_{10}$ [35–40]. This directly leads to a strong nearest neighbor (NN) exchange interaction $J_1$ within each trimer [see Fig. 1(a)]. Another intra-trimer interaction is the third NN term $J_3$, which can be realized by the superexchange path through the Ir2 ion. The Ir1 ions are also connected through the second NN interaction $J_2$, forming zig-zag chains along the crystalline $c$ direction. All other magnetic interactions can be ignored due to the long bond lengths and unfavorable hopping trajectories. Considering the expectation of appreciable magnetic exchange and the lack of any obvious magnetic frustration, this material would be expected to be a long-range ordered antiferromagnet. Previous transport and magnetization studies found no magnetic order down to 0.2 K despite a Curie-Weiss temperature up to -766 K [25]. In contrast, the material shows a linear behavior in the low-temperature magnetic heat capacity [25], resembling a gapless QSL [41, 42]. In fact, the ground state is rather susceptible to perturbations including sample growth conditions and chemical doping [25–27]. The origin of the highly suppressed magnetic order and fragile ground state remains puzzling and cannot be solved without direct measurements of the magnetic excitation spectrum.

In this paper, we use resonant inelastic x-ray scattering (RIXS) at the Ir $L_3$-edge and resonant elastic x-ray scattering (REXS) at the O $K$-edge to study the magnetic properties of $Ba_4Ir_3O_{10}$. For comparison, we also measure the isovalently doped $(Ba_{1-x}Sr_x)_4Ir_3O_{10}$

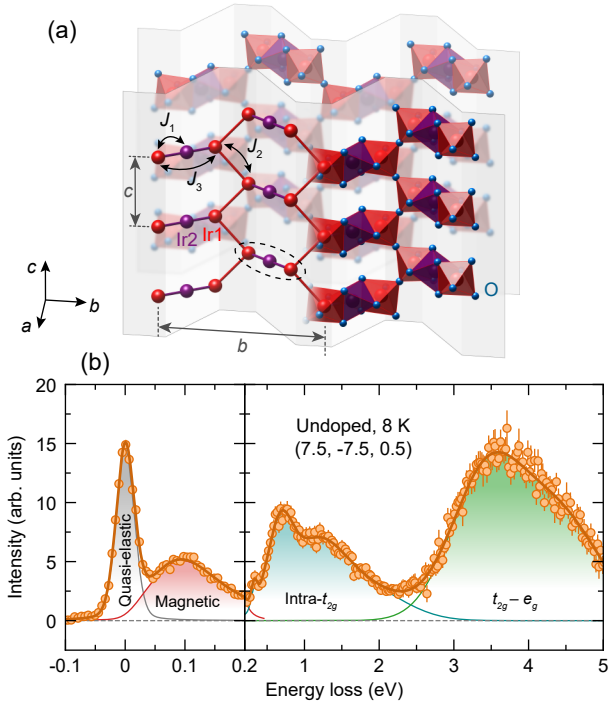


FIG. 1. (a) Crystal structure of $Ba_4Ir_3O_{10}$. The material contains two symmetry-inequivalent Ir ions: Ir1 and Ir2, occupying the outer and middle sites of the trimers (black dashed ellipse), respectively. $J_n$ where $n = 1, 2, 3$ denotes magnetic interactions for the first, second, and third nearest Ir neighbors. The barium ions are not shown. (b) Representative RIXS spectrum of $Ba_4Ir_3O_{10}$ at the Ir $L_3$-edge with a constant background subtracted. The circles represent the data and the different lines with shaded areas indicate the fitting results of different components, the summation of which gives the dark orange curve. Error bars represent 1 standard deviation based on Poisson statistics.

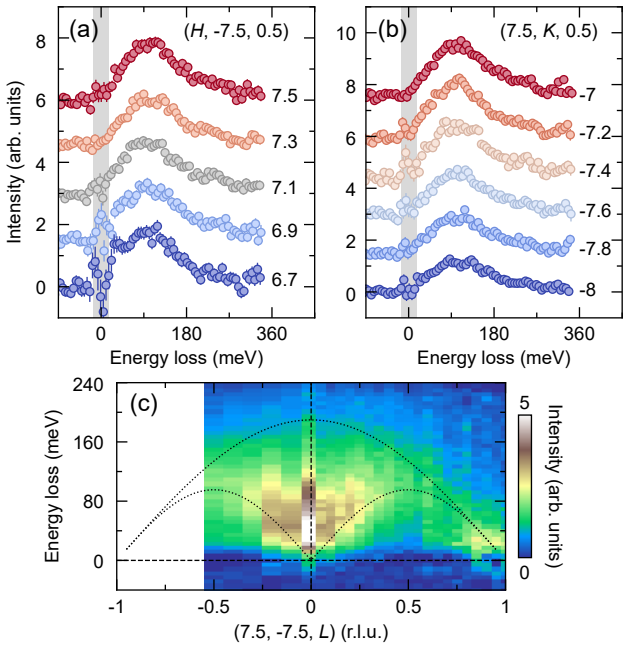


FIG. 2. One-dimensional spinons in undoped $Ba_4Ir_3O_{10}$ at 8 K. (a), (b) Magnetic excitations at different $\boldsymbol{Q}$ along $H$ and $K$ directions, respectively, showing essentially dispersionless behavior. All the RIXS spectra in the text are presented with the constant background, quasi-elastic line and high-energy $dd$ excitations subtracted to highlight the magnetic contributions [43]. The vertical gray bars indicate the quasi-elastic regime, the widths of which represent the energy resolution. The values of $H/K$ are indicated for each curve and the spectra are shifted along the $y$ axis for clarity. (c) Colorplot of the magnetic excitations along the $L$ direction. The dotted lines are the calculated excitation boundaries of an AFM spin-1/2 chain with $J_{\rm chain} = 55$ meV and $\Delta = 1.3$. The dashed lines are guides to the eye.

($x$=0.02), in which a small amount of Sr doping surprisingly triggers magnetic order below 130 K. 1D continuous spinon excitations are discovered in undoped $Ba_4Ir_3O_{10}$ which can be well-described by a spin-1/2 XXZ AFM chain with small Ising-like anisotropy. In contrast, $(Ba_{1-x}Sr_x)_4Ir_3O_{10}$ shows magnetic order with propagation vector of (0.5, 0, 0), and a comparably sharp dispersion, which remains 1D like down to base temperature. Through exact diagonalization (ED) calculations, we show that the zig-zag chains retained by $J_2$ are effectively decoupled at a critical point triggered by the competition between the inter-chain interactions $J_1$ and $J_3$, the balance of which can be easily tipped by perturbations.

RIXS data were collected at the Ir $L_3$-edge with a horizontal scattering plane and $\pi$ polarization and energy resolution of about 32 meV [43]. Wavevectors throughout the manuscript are defined using standard reciprocal lattice units (r.l.u.) notation as $\boldsymbol{Q} = H\mathbf{a}^* + K\mathbf{b}^* + L\mathbf{c}^*$ based on lattice constants $a$ =7.2545 Å, $b$ =13.192 Å, $c$ =5.7737 Å, $\alpha = \gamma = 90°$, $\beta = 113.513°$.

Figure 1(b) displays a representative Ir $L_3$-edge RIXS spectrum at 11.215 keV composed of a quasi-elastic peak, low-energy magnetic excitations, and high-energy $dd$ excitations of both intra-$t_{2g}$ orbitals and from $t_{2g}$ to $e_g$ orbitals. The overall form of the spectrum is consistent with expectations for Ir $5d^5$ materials [44, 45]. We further checked for possible intra-trimer charge disproportionation via bond valence sum analysis and found it to be negligible [43]. To separate the spectral components we fit the spectra with different functions. The quasi-elastic peak can be represented by a pseudo-Voigt profile with a width dominated by the energy resolution. The low symmetry of $Ba_4Ir_3O_{10}$ implies that the magnetic and crystal field excitations are unlikely to have theoretically rigorous analytical forms. We find that phenomenological forms of a damped harmonic oscillator convoluted with the resolution and a manifold of pseudo-Voigts can represent the magnetic and $dd$ excitations respectively, as shown by the fit lines in Fig. 1(b) [43]. These phe-

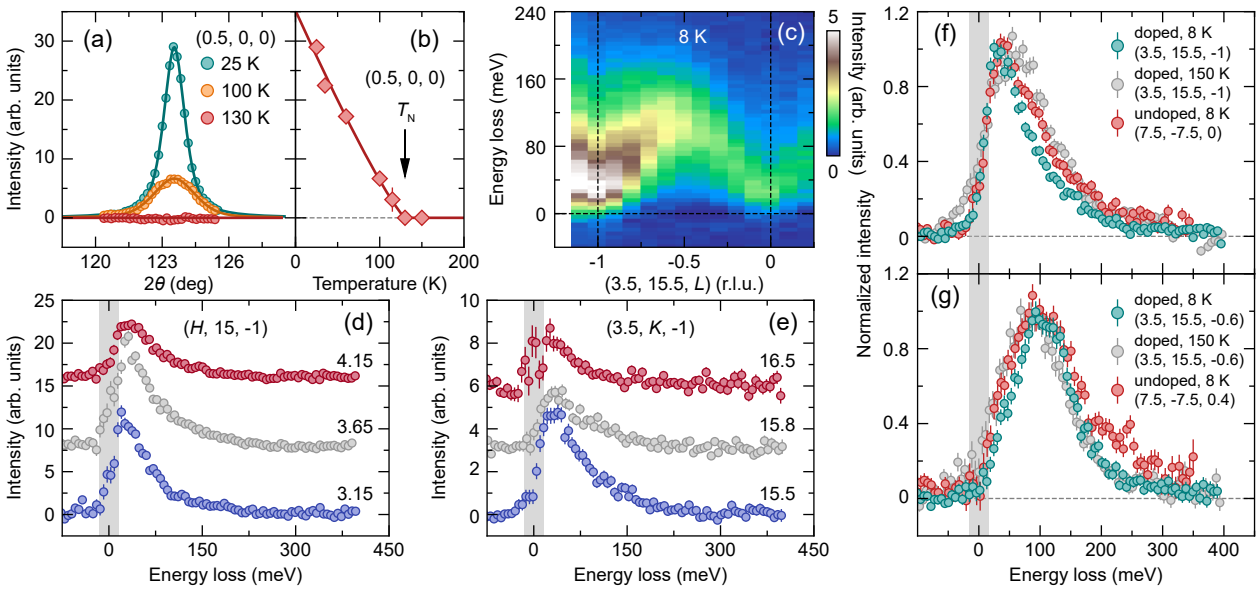


FIG. 3. Magnetic order and spin dynamics in doped $(Ba_{1-x}Sr_x)_4Ir_3O_{10}$ ($x = 0.02$) and comparison with undoped $Ba_4Ir_3O_{10}$. (a) Background subtracted magnetic Bragg peaks at $\boldsymbol{Q}$=(0.5, 0, 0), detected at the O $K$-edge with different temperatures in $(Ba_{1-x}Sr_x)_4Ir_3O_{10}$. The solid lines are the fitting results using pseudo-Voigt profiles [43]. (b) Temperature dependence of the fitted peak height. The magnetic transition takes place at $T_N$=130 K. The solid and dashed lines are guides to the eye. (c)-(e) Magnetic excitation spectra of $(Ba_{1-x}Sr_x)_4Ir_3O_{10}$ at 8 K with different $\boldsymbol{Q}$ along $L$, $H$ and $K$ directions, respectively. (f), (g) Magnetic excitation spectra at different temperatures for $Ba_4Ir_3O_{10}$ and $(Ba_{1-x}Sr_x)_4Ir_3O_{10}$ samples. The intensities are normalized according to their maximum values. Note that (3.5, 15.5, -1) and (7.5, -7.5, 0) are symmetric regarding the chain direction. The observed phase shift in the spinon spectrum with respect to $L$ arises from zone folding caused by the inter-chain interactions and the sampling of different chains with changes in $\boldsymbol{Q}$ [9]. The same applies to (3.5, 15.5, -0.6) and (7.5, -7.5, 0.4). The dashed lines are guides to the eye and the quasi-elastic regime is indicated by the vertical gray bars.

nomenological forms for the quasi-elastic line and intra-$t_{2g}$ excitations will be used later to isolate the magnetic scattering which is the main focus of this paper.

We start with the magnetic excitations in undoped $Ba_4Ir_3O_{10}$ along different momentum directions. Our sample comes from the same batch studied in Ref. [25] that show no magnetic transition down to 0.2 K. As plotted in Fig. 2(a), (b), both the energies and lineshapes are essentially dispersionless in ($H$, 0, 0) and (0, $K$, 0) directions. In contrast, dispersive excitations are revealed along the $L$ direction [Fig. 2(c)]. Intriguingly, the excitations are very broad along the energy loss axis, distinct from sharp spin waves, rather resembling the magnetic continuum consistent with spinons. A gap-like feature is observed with intensity maximum around 40 meV, consistent with the anisotropy revealed by magnetization [25]. Considering the 1D character of the dispersion, we propose a spin-1/2 XXZ AFM chain Hamiltonian

$$\mathcal{H} = J_{\text{chain}} \sum_{\langle ij \rangle} [S_i^x S_j^x + S_i^y S_j^y + \Delta S_i^z S_j^z] \qquad (1)$$

where $J_{\text{chain}}$ is the NN intra-chain interactions, which corresponds to $J_2$ in our case connecting the Ir1 atoms, $\langle ij \rangle$ denotes bond sums along the chain, and $\Delta$ controls the interaction anisotropy. We calculated the zero temperature two-spinon response with $J_{\text{chain}} = 55$ meV and $\Delta = 1.3$ and plot the result in Fig. 2(c) and Fig. S5 [43, 46]. This provides a satisfactory description of all the major features of the data, indicating that, despite the 2D structure of $Ba_4Ir_3O_{10}$, its magnetic dynamics can be well described by the continuous spinon excitations of 1D AFM chains.

To test the fragility of the QSL state, we turn to the isovalently doped $(Ba_{1-x}Sr_x)_4Ir_3O_{10}$ ($x = 0.02$) which has been previously reported to show a magnetic transition below $T_N$=130 K [25]. We used O $K$-edge REXS measurements to test for the presence of order and reveal a magnetic Bragg peak at $\boldsymbol{Q}$=(0.5, 0, 0) [Fig. 3(a), (b)], which disappears above $T_N$=130 K, consistent with the thermodynamic results [25]. Regarding the magnetic excitations, similar with the undoped $Ba_4Ir_3O_{10}$, no dispersion can be distinguished along $H$ and $K$ directions in $(Ba_{1-x}Sr_x)_4Ir_3O_{10}$, while clear $\boldsymbol{Q}$ dependence is discovered along $L$ direction at 8 K [Fig. 3(c)-(e)]. A gap-like feature is also observed, consistent with its slight Ising-type anisotropy. However, further analysis of the gap structure, and its correspondence to the heat capacity data, is impeded by the limited energy resolution here. Above $T_N$, the excitations become broader and less dispersive [Fig. 3(f), (g)]. The flattening of the dispersion is in line with the Ising spin nature.

It has been theoretically proposed that the oxygen-

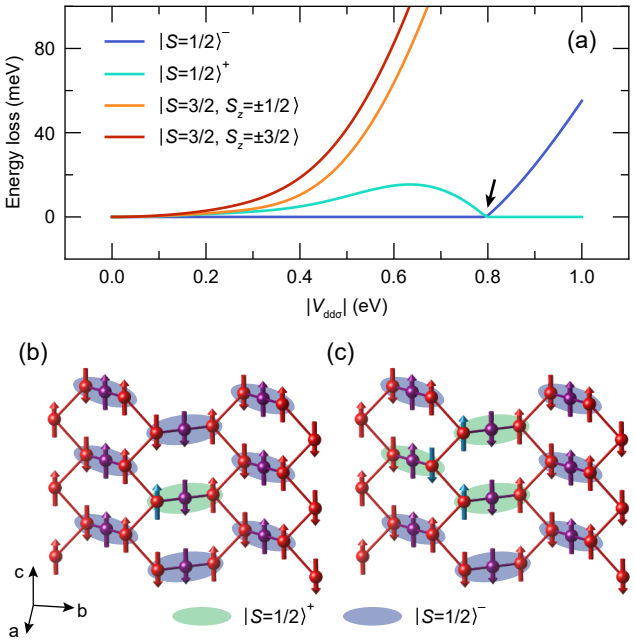


FIG. 4. Effective chain decoupling. (a) Low-energy spectrum of the three-Ir-site cluster model as a function of inter-site $d$–$d$ hopping [43]. The black arrow highlights the critical point where the $|S = 1/2\rangle^+$ and $|S = 1/2\rangle^-$ doublets are degenerate. (b) During the RIXS process, one Ir spin is flipped (cyan arrow), changing the trimer state at low energies and creating two spinons (domain walls). (c) The spinons can propagate in the zigzag chain along $c$ direction by flipping the neighboring spins.

mediated electronic hopping between face-sharing Ir octahedra can be extremely weak under certain circumstances [47], leading to vanishing $J_1$ superexchange parameters, naturally decoupling the zig-zag chains running along $c$ direction in $Ba_4Ir_3O_{10}$. However, this weak coupling model does not take into account the direct hoppings between the neighboring Ir ions which tend to be significant for face-sharing octahedra [31–40]. Indeed, the Bonner-Fisher peak in the susceptibility expected for 1D systems [48, 49], is absent in $Ba_4Ir_3O_{10}$ [25]. Furthermore, compared with undoped $Ba_4Ir_3O_{10}$, the excitations in magnetically ordered $(Ba_{1-x}Sr_x)_4Ir_3O_{10}$ have similarly shaped dispersion but are somewhat sharper in energy [Fig. 3(f), (g)]. This behavior differs from that expected for the weak coupling model, where the weak inter-chain coupling leads to multiple bound triplon states in addition to the spinon continuum [9, 24, 50, 51]. Such inconsistency leads us to another explanation, a strong coupling model [52, 53], where the intra-trimer AFM interactions $J_1$ and $J_3$ are substantial and compete with each other, effectively decoupling the chains.

To understand the origin of the frustration between $J_1$ and $J_3$, we make use of cluster ED calculations utilizing the EDRIXS software [54]. We represent the trimer units in $Ba_4Ir_3O_{10}$ using a cluster model with three Ir sites with Coulomb interactions and inter-atomic $d$-$d$ hopping explicitly taken into account through Slater-Koster parameterization [43]. For each Ir site with a nominal $5d^5$ configuration, the ground state is an $S_{\rm eff} = 1/2$ doublet. These $S_{\rm eff} = 1/2$ states recombine in the cluster to yield four Kramers doublets: an antisymmetric doublet $|S = 1/2\rangle^-$, a symmetric doublet $|S = 1/2\rangle^+$, and a high-spin multiplet $|S = 3/2\rangle$ which can further split into $|S = 3/2, S_z = \pm 1/2\rangle$ and $|S = 3/2, S_z = \pm 3/2\rangle$ in the presence of anisotropic interactions [43]. As shown in Fig. 4(a), with increasing inter-Ir-site hopping, the energies of $|S = 3/2, S_z = \pm 1/2\rangle$ and $|S = 3/2, S_z = \pm 3/2\rangle$ increase monotonically. The fact that the $|S = 3/2, S_z = \pm 3/2\rangle$ doublet lies at higher energy indicates Ising-like anisotropy for the intra-trimer interactions. In contrast, $|S = 1/2\rangle^-$ and $|S = 1/2\rangle^+$ show strong competition and the ground state switches between these two doublets at a critical point of $V_{dd\sigma} \approx 0.8$ eV.

The presence of the critical point directly leads to the effective decoupling of the spin chains. Assuming an $|S = 1/2\rangle^-$ ground state for all the trimers (the real ground state is a superposition of $|S = 1/2\rangle^+$ and $|S = 1/2\rangle^-$ at the critical point), the RIXS process leads to a single spin flip at one of the Ir sites [Fig. 4(b)], which at low energies turns the corresponding trimer from $|S = 1/2\rangle^-$ to $|S = 1/2\rangle^+$, leaving two spinons (domain walls) in the zigzag spin chain. As the spinons propagate along the chain, the neighboring spins are flipped, switching the trimers between $|S = 1/2\rangle^-$ and $|S = 1/2\rangle^+$ [Fig. 4(c)]. At the critical point, as the $|S = 1/2\rangle^-$ and $|S = 1/2\rangle^+$ doublets are degenerate, such events have no energy cost so that the spinons are deconfined and can propagate freely. Thus, the properties of undoped $Ba_4Ir_3O_{10}$ are naturally explained if it sits right at the critical point, resulting in emergent 1D behavior and continuous excitations observed in RIXS spectra. The delicate balance between competing interactions can be disrupted easily. In $(Ba_{1-x}Sr_x)_4Ir_3O_{10}$, the isovalent Sr doping leads to small structural changes and drives the system slightly away from the critical point so that the spinons become confined since the energy cost to switch between $|S = 1/2\rangle^-$ and $|S = 1/2\rangle^+$ doublets is no longer zero. Such behavior differs from the conventional doping effect where the dopants could enhance disorder and randomness, which tends to suppress magnetic order and promote glassy physics [55]. It should be noted that the Ising-like anisotropy in $(Ba_{1-x}Sr_x)_4Ir_3O_{10}$ makes it free from the constraints of Mermin-Wagner theorem which requires a continuous symmetry. Thus, magnetic order does not necessarily imply finite inter-layer coupling, although our diffraction measurements show $H$-axis correlations proving that inter-layer coupling is present. A recent REXS experiment reports a 25 K magnetic transition in the undoped $Ba_4Ir_3O_{10}$ with a similar propagation vector as we found in the doped $(Ba_{1-x}Sr_x)_4Ir_3O_{10}$ [27]. The origin of this discrepancy is unclear, but it could

indicate enhanced disorder.

The strong coupling model puts $Ba_4Ir_3O_{10}$ in between the 1D spin chains and 2D QSLs. Although its magnetic dynamics behave as 1D spinon excitations, the underlying magnetism is mostly 2D. Consequently, some of the characteristic features for a 1D system are missing such as the Bonner-Fisher peak in susceptibility and bound state upon ordering. The 1D behavior is caused by the emergent dimensional reduction due to magnetic frustration, which has also been reported in other materials [56]. This raises an interesting question of whether the properties relevant to 2D QSLs are preserved in this case, which is yet to be explored. Measurements of quantum entanglement, such as entanglement witnesses, could prove useful in this regard [22].

In summary, we use RIXS to show that emergent 1D spinon excitations can arise from the 2D magnetism in $Ba_4Ir_3O_{10}$ due to the frustrated inter-chain (intra-trimer) interactions. The highly suppressed magnetic order can be easily recovered by disturbing the subtle balance of the frustration, confining the spinons into magnons. Although prior work has speculated that $Ba_4Ir_3O_{10}$ could be either a Luttinger liquid QSL or a 2D QSL such as a spinon Fermi surface states [25], the data here are the first evidence of a 1D spinon continuum in $Ba_4Ir_3O_{10}$. These results indicate that, instead of forming an isotropic QSL state, magnetic frustration can effectively reduce the system dimension, suppressing the magnetic order and realizing deconfined spinons in a unique way.

We thank Emil Bozin and Kemp Plumb for insightful conversations. Work at Brookhaven National Laboratory was supported by the U.S. Department of Energy, Office of Science, Office of Basic Energy Sciences. G.C. acknowledges NSF support via grant DMR 1903888. This research used resources of the Advanced Photon Source, a U.S. Department of Energy (DOE) Office of Science User Facility at Argonne National Laboratory and is based on research supported by the U.S. DOE Office of Science-Basic Energy Sciences, under Contract No. DE-AC02-06CH11357. This research used resources at the Coherent Soft X-Ray and In Situ and Resonant Hard X-ray Studies beamline of the National Synchrotron Light Source II, a U.S. Department of Energy (DOE) Office of Science User Facility operated for the DOE Office of Science by Brookhaven National Laboratory under Contract No. DE-SC0012704.

* yshen@bnl.gov
† mdean@bnl.gov

[1] P. W. Anderson, Resonating valence bonds: A new kind of insulator?, Materials Research Bulletin **8**, 153 (1973).
[2] P. W. Anderson, The resonating valence bond state in $La_2CuO_4$ and superconductivity, Science **235**, 1196 (1987).
[3] L. Balents, Spin liquids in frustrated magnets, Nature **464**, 199 (2010).
[4] L. Savary and L. Balents, Quantum spin liquids: a review, Reports on Progress in Physics **80**, 016502 (2017).
[5] Y. Zhou, K. Kanoda, and T.-K. Ng, Quantum spin liquid states, Reviews of Modern Physics **89**, 025003 (2017).
[6] C. Broholm, R. Cava, S. Kivelson, D. Nocera, M. Norman, and T. Senthil, Quantum spin liquids, Science **367**, 263 (2020).
[7] B. Lake, D. A. Tennant, C. D. Frost, and S. E. Nagler, Quantum criticality and universal scaling of a quantum antiferromagnet, Nature Materials **4**, 329 (2005).
[8] M. Mourigal, M. Enderle, A. Klopperpieper, J.-S. Caux, A. Stunault, and H. M. Rønnow, Fractional spinon excitations in the quantum Heisenberg antiferromagnetic chain, Nature Physics **9**, 435 (2013).
[9] A. K. Bera, B. Lake, F. H. L. Essler, L. Vanderstraeten, C. Hubig, U. Schollwöck, A. T. M. N. Islam, A. Schneidewind, and D. L. Quintero-Castro, Spinon confinement in a quasi-one-dimensional anisotropic Heisenberg magnet, Physical Review B **96**, 054423 (2017).
[10] Q. Faure, S. Takayoshi, S. Petit, V. Simonet, S. Raymond, L.-P. Regnault, M. Boehm, J. S. White, M. Månsson, C. Rüegg, P. Lejay, B. Canals, T. Lorenz, S. C. Furuya, T. Giamarchi, and B. Grenier, Topological quantum phase transition in the Ising-like antiferromagnetic spin chain $BaCo_2V_2O_8$, Nature Physics **14**, 716 (2018).
[11] Q. Faure, S. Takayoshi, V. Simonet, B. Grenier, M. Månsson, J. S. White, G. S. Tucker, C. Rüegg, P. Lejay, T. Giamarchi, and S. Petit, Tomonaga-Luttinger liquid spin dynamics in the quasi-one-dimensional Ising-like antiferromagnet $BaCo_2V_2O_8$, Physical Review Letters **123**, 027204 (2019).
[12] J. Schlappa, K. Wohlfeld, K. J. Zhou, M. Mourigal, M. W. Haverkort, V. N. Strocov, L. Hozoi, C. Monney, S. Nishimoto, S. Singh, A. Revcolevschi, J. S. Caux, L. Patthey, H. M. Rnnow, J. van den Brink, and T. Schmitt, Spinorbital separation in the quasi-one-dimensional mott insulator $Sr_2CuO_3$, Nature **485**, 82 (2012).
[13] V. Bisogni, K. Wohlfeld, S. Nishimoto, C. Monney, J. Trinckauf, K. Zhou, R. Kraus, K. Koepernik, C. Sekar, V. Strocov, B. Büchner, T. Schmitt, J. van den Brink, and J. Geck, Orbital control of effective dimensionality: From spin-orbital fractionalization to confinement in the anisotropic ladder system $CaCu_2O_3$, Physical Review Letters **114**, 096402 (2015).
[14] U. Kumar, A. Nag, J. Li, H. C. Robarts, A. C. Walters, M. García-Fernández, R. Saint-Martin, A. Revcolevschi, J. Schlappa, T. Schmitt, S. Johnston, and K.-J. Zhou, Unraveling higher-order contributions to spin excitations probed using resonant inelastic x-ray scattering, Phys. Rev. B **106**, L060406 (2022).
[15] M. Rossi, P. Marabotti, Y. Hirata, G. Monaco, M. Krisch, K. Ohgushi, K. Wohlfeld, J. van den Brink, and M. Moretti Sala, A $j_{\text{eff}} = 1/2$ pseudospinon continuum in $CaIrO_3$, The European Physical Journal Plus **135**, 676 (2020).
[16] X.-G. Wen, Quantum orders and symmetric spin liquids, Physical Review B **65**, 165113 (2002).
[17] L. B. Ioffe, M. V. Feigel'man, A. Ioselevich, D. Ivanov, M. Troyer, and G. Blatter, Topologically protected quan-

tum bits using Josephson junction arrays, Nature **415**, 503 (2002).
[18] T.-H. Han, J. S. Helton, S. Chu, D. G. Nocera, J. A. Rodriguez-Rivera, C. Broholm, and Y. S. Lee, Fractionalized excitations in the spin-liquid state of a kagome-lattice antiferromagnet, Nature **492**, 406 (2012).
[19] Y. Shen, Y.-D. Li, H. Wo, Y. Li, S. Shen, B. Pan, Q. Wang, H. C. Walker, P. Steffens, M. Boehm, Y. Hao, D. L. Quintero-Castro, L. W. Harriger, M. D. Frontzek, L. Hao, S. Meng, Q. Zhang, G. Chen, and J. Zhao, Evidence for a spinon fermi surface in a triangular-lattice quantum-spin-liquid candidate, Nature **540**, 559 (2016).
[20] B. Gao, T. Chen, D. W. Tam, C.-L. Huang, K. Sasmal, D. T. Adroja, F. Ye, H. Cao, G. Sala, M. B. Stone, C. Baines, J. A. T. Verezhak, H. Hu, J.-H. Chung, X. Xu, S.-W. Cheong, M. Nallaiyan, S. Spagna, M. B. Maple, A. H. Nevidomskyy, E. Morosan, G. Chen, and P. Dai, Experimental signatures of a three-dimensional quantum spin liquid in effective spin-1/2 $Ce_2Zr_2O_7$ pyrochlore, Nature Physics **15**, 1052 (2019).
[21] L. Martinelli, D. Betto, K. Kummer, R. Arpaia, L. Braicovich, D. Di Castro, N. B. Brookes, M. Moretti Sala, and G. Ghiringhelli, Fractional spin excitations in the infinite-layer cuprate $cacuo_2$, Phys. Rev. X **12**, 021041 (2022).
[22] A. O. Scheie, E. A. Ghioldi, J. Xing, J. A. M. Paddison, N. E. Sherman, M. Dupont, D. Abernathy, D. M. Pajerowski, S.-S. Zhang, L. O. Manuel, A. E. Trumper, C. D. Pemmaraju, A. S. Sefat, D. S. Parker, T. P. Devereaux, J. E. Moore, C. D. Batista, and D. A. Tennant, Witnessing quantum criticality and entanglement in the triangular antiferromagnet $KYbSe_2$, arXiv e-prints , arXiv:2109.11527 (2021).
[23] A. Banerjee, J. Yan, J. Knolle, C. A. Bridges, M. B. Stone, M. D. Lumsden, D. G. Mandrus, D. A. Tennant, R. Moessner, and S. E. Nagler, Neutron scattering in the proximate quantum spin liquid $\alpha$-$RuCl_3$, Science **356**, 1055 (2017).
[24] M. Kohno, O. A. Starykh, and L. Balents, Spinons and triplons in spatially anisotropic frustrated antiferromagnets, Nature Physics **3**, 790 (2007).
[25] G. Cao, H. Zheng, H. Zhao, Y. Ni, C. A. Pocs, Y. Zhang, F. Ye, C. Hoffmann, X. Wang, M. Lee, M. Hermele, and I. Kimchi, Quantum liquid from strange frustration in the trimer magnet $Ba_4Ir_3O_{10}$, npj Quantum Materials **5**, 26 (2020).
[26] G. Cao, H. Zhao, B. Hu, N. Pellatz, D. Reznik, P. Schlottmann, and I. Kimchi, Quest for quantum states via field-altering technology, npj Quantum Materials **5**, 83 (2020).
[27] X. Chen, Y. He, S. Wu, Y. Song, D. Yuan, E. Bourret-Courchesne, J. P. C. Ruff, Z. Islam, A. Frano, and R. J. Birgeneau, Structural and magnetic transitions in the planar antiferromagnet $Ba_4Ir_3O_{10}$, Physical Review B **103**, 224420 (2021).
[28] A. Sokolik, S. Hakani, S. Roy, N. Pellatz, H. Zhao, G. Cao, I. Kimchi, and D. Reznik, Spinons and damped phonons in spin-1/2 quantum-liquid $Ba_4Ir_3O_{10}$ observed by Raman scattering, arXiv e-prints , arXiv:2110.15916 (2021).
[29] K. E. Stitzer, M. D. Smith, and H.-C. zur Loye, Crystal growth, structure determination and magnetic properties of $Ba_4Ir_3O_{10}$ and $Ba_4(Co_{0.4}Ir_{0.6})Ir_2O_{10}$, Journal of Alloys and Compounds **338**, 104 (2002).
[30] R. Wyckoff, *Crystal Structures* (Wiley, 1963).
[31] I. Terasaki, S. Ito, T. Igarashi, S. Asai, H. Taniguchi, R. Okazaki, Y. Yasui, K. Kobayashi, R. Kumai, H. Nakao, and Y. Murakami, Novel charge ordering in the trimer iridium oxide $BaIrO_3$, Crystals **6**, 27 (2016).
[32] R. Okazaki, S. Ito, K. Tanabe, H. Taniguchi, Y. Ikemoto, T. Moriwaki, and I. Terasaki, Spectroscopic signature of trimer Mott insulator and charge disproportionation in $BaIrO_3$, Physical Review B **98**, 205131 (2018).
[33] M. Ye, H.-S. Kim, J.-W. Kim, C.-J. Won, K. Haule, D. Vanderbilt, S.-W. Cheong, and G. Blumberg, Covalency-driven collapse of strong spin-orbit coupling in face-sharing iridium octahedra, Physical Review B **98**, 201105 (2018).
[34] Y. Wang, R. Wang, J. Kim, M. H. Upton, D. Casa, T. Gog, G. Cao, G. Kotliar, M. P. M. Dean, and X. Liu, Direct detection of dimer orbitals in $Ba_5AlIr_2O_{11}$, Physical Review Letters **122**, 106401 (2019).
[35] Y. Klein, G. Rousse, F. Damay, F. Porcher, G. Andr, and I. Terasaki, Antiferromagnetic order and consequences on the transport properties of $Ba_4Ru_3O_{10}$, Physical Review B **84**, 054439 (2011).
[36] S. V. Streltsov and D. I. Khomskii, Unconventional magnetism as a consequence of the charge disproportionation and the molecular orbital formation in $Ba_4Ru_3O_{10}$, Physical Review B **86**, 064429 (2012).
[37] T. Igarashi, Y. Nogami, Y. Klein, G. Rousse, R. Okazaki, H. Taniguchi, Y. Yasui, and I. Terasaki, X-ray crystal structure analysis and Ru valence of $Ba_4Ru_3O_{10}$ single crystals, Journal of the Physical Society of Japan **82**, 104603 (2013).
[38] G. Radtke, A. Saúl, Y. Klein, and G. Rousse, Magnetism of $Ba_4Ru_3O_{10}$ revealed by density functional calculations: Structural trimers behaving as coupled magnetic dimers, Physical Review B **87**, 054436 (2013).
[39] T. Igarashi, R. Okazaki, H. Taniguchi, Y. Yasui, and I. Terasaki, Effects of the Ir impurity on the thermodynamic and transport properties of $Ba_4Ru_3O_{10}$, Journal of the Physical Society of Japan **84**, 094601 (2015).
[40] J. Sannigrahi, A. Paul, A. Banerjee, D. Khalyavin, A. D. Hillier, K. Yokoyama, A. K. Bera, M. R. Lees, I. Dasgupta, S. Majumdar, and D. T. Adroja, Orbital effects and Affleck-Haldane-type spin dimerization in $Ba_4Ru_3O_{10}$, Physical Review B **103**, 144431 (2021).
[41] S. Yamashita, Y. Nakazawa, M. Oguni, Y. Oshima, H. Nojiri, Y. Shimizu, K. Miyagawa, and K. Kanoda, Thermodynamic properties of a spin-1/2 spin-liquid state in a $\kappa$-type organic salt, Nature Physics **4**, 459 (2008).
[42] S. Yamashita, T. Yamamoto, Y. Nakazawa, M. Tamura, and R. Kato, Gapless spin liquid of an organic triangular compound evidenced by thermodynamic measurements, Nature Communications **2**, 275 (2011).
[43] See Supplemental Material at [URL will be inserted by publisher] for bond valence sum analysis, additional details of the X-ray measurements and fittings, which also includes references [57–62].
[44] J. Kim, D. Casa, M. H. Upton, T. Gog, Y.-J. Kim, J. F. Mitchell, M. van Veenendaal, M. Daghofer, J. van den Brink, G. Khaliullin, and B. J. Kim, Magnetic excitation spectra of $Sr_2IrO_4$ probed by resonant inelastic x-ray scattering: Establishing links to cuprate superconductors, Physical Review Letters **108**, 177003 (2012).
[45] X. Liu, V. M. Katukuri, L. Hozoi, W.-G. Yin, M. P. M. Dean, M. H. Upton, J. Kim, D. Casa, A. Said, T. Gog,

T. F. Qi, G. Cao, A. M. Tsvelik, J. van den Brink, and J. P. Hill, Testing the validity of the strong spin-orbit-coupling limit for octahedrally coordinated iridate compounds in a model system $Sr_3CuIrO_6$, Physical Review Letters **109**, 157401 (2012).

[46] J.-S. Caux, J. Mossel, and I. P. Castillo, The two-spinon transverse structure factor of the gapped Heisenberg antiferromagnetic chain, Journal of Statistical Mechanics: Theory and Experiment **2008**, P08006 (2008).

[47] K. I. Kugel, D. I. Khomskii, A. O. Sboychakov, and S. V. Streltsov, Spin-orbital interaction for face-sharing octahedra: Realization of a highly symmetric SU(4) model, Physical Review B **91**, 155125 (2015).

[48] D. C. Johnston, R. K. Kremer, M. Troyer, X. Wang, A. Klmper, S. L. Budko, A. F. Panchula, and P. C. Canfield, Thermodynamics of spin $s = 1/2$ antiferromagnetic uniform and alternating-exchange Heisenberg chains, Physical Review B **61**, 9558 (2000).

[49] Y. Savina, O. Bludov, V. Pashchenko, S. L. Gnatchenko, P. Lemmens, and H. Berger, Magnetic properties of the antiferromagnetic spin-$\frac{1}{2}$ chain system $\beta$-$TeVO_4$, Physical Review B **84**, 104447 (2011).

[50] R. Coldea, D. A. Tennant, E. M. Wheeler, E. Wawrzynska, D. Prabhakaran, M. Telling, K. Habicht, P. Smeibidl, and K. Kiefer, Quantum criticality in an Ising chain: Experimental evidence for emergent $E_8$ symmetry, Science **327**, 177 (2010).

[51] M. Mena, N. Hnni, S. Ward, E. Hirtenlechner, R. Bewley, C. Hubig, U. Schollwck, B. Normand, K. W. Krmer, D. F. McMorrow, and C. Rüegg, Thermal control of spin excitations in the coupled ising-chain material $RbCoCl_3$, Physical Review Letters **124**, 257201 (2020).

[52] W. Yin, Frustration-driven unconventional phase transitions at finite temperature in a one-dimensional ladder ising model, arXiv e-prints , arXiv:2006.08921 (2020).

[53] A. Weichselbaum, W. Yin, and A. M. Tsvelik, Dimerization and spin decoupling in a two-leg Heisenberg ladder with frustrated trimer rungs, Physical Review B **103**, 125120 (2021).

[54] EDRIXS website, `https://github.com/NSLS-II/edrixs`, accessed: 2021-09-27.

[55] J. A. Mydosh, *Spin Glasses: An Experimental Introduction* (CRC Press, 1993).

[56] R. Okuma, M. Kofu, S. Asai, M. Avdeev, A. Koda, H. Okabe, M. Hiraishi, S. Takeshita, K. M. Kojima, R. Kadono, T. Masuda, K. Nakajima, and Z. Hiroi, Dimensional reduction by geometrical frustration in a cubic antiferromagnet composed of tetrahedral clusters, Nature Communications **12**, 4382 (2021).

[57] X. Liu, M. P. M. Dean, J. Liu, S. G. Chiuzbăian, N. Jaouen, A. Nicolaou, W. G. Yin, C. R. Serrao, R. Ramesh, and H. Ding, Probing single magnon excitations in $Sr_2IrO_4$ using O K-edge resonant inelastic x-ray scattering, Journal of Physics: Condensed Matter **27**, 202202 (2015).

[58] D. I. Brown, *The Chemical Bond in Inorganic Chemistry: The Bond Valence Model* (Oxford University Press, 2006).

[59] Bond valence parameters, `https://www.iucr.org/resources/data/data-sets/bond-valence-parameters`, accessed: 2021-11-15.

[60] Y. Shen, G. Fabbris, H. Miao, Y. Cao, D. Meyers, D. G. Mazzone, T. A. Assefa, X. M. Chen, K. Kisslinger, D. Prabhakaran, A. T. Boothroyd, J. M. Tranquada, W. Hu, A. M. Barbour, S. B. Wilkins, C. Mazzoli, I. K. Robinson, and M. P. M. Dean, Charge condensation and lattice coupling drives stripe formation in nickelates, Physical Review Letters **126**, 177601 (2021).

[61] O. K. Andersen, W. Klose, and H. Nohl, Electronic structure of Chevrel-phase high-critical-field superconductors, Physical Review B **17**, 1209 (1978).

[62] I. Pérez Castillo, The exact two-spinon longitudinal dynamical structure factor of the anisotropic XXZ model, arXiv e-prints , arXiv:2005.10729 (2020).